Design and Characterization of a UWB Slot Antenna Optimized for Radiation in Human Tissue

Mario Leib, Michael Frei, Dietmar Sailer, and Wolfgang Menzel

University of Ulm, Microwave Techniques, Albert-Einstein-Allee 41, 89081 Ulm, Germany
Email: mario.leib@uni-ulm.de

***Abstract*—Ultra-wideband (UWB) short-range communication systems are valuable in medical technology, particularly for implanted devices, due to their low power consumption, low cost, and high-data rates. Hence, antennas suitable for implantation in the human body are desired. The focus of this publication is on the design of a small planar UWB slot antenna, optimized for operation in human tissue. The antenna is fed by a triplate line and operates in the frequency range 3.1 GHz–10.6 GHz. The characterization of the antenna is performed in selected tissue mimic liquids, and the obtained radiation diagram shows a desired uniform characteristic over frequency. The measured mean antenna gain is 3.8 dBi. Besides the antenna design, the general properties of human tissue, the lossy phantom liquids, and the measurement setup for the radiation in human tissue are briefly discussed within this paper.**

***Index Terms*—slot antenna, ultra-wideband (UWB), biological tissue, antenna characterization, lossy media, biotelemetry**

I. Introduction

In medical technology, wireless data transmission with implanted devices is an emerging topic. A major application is the communication with cardiac pacemakers. There, devices operating in the implant communication service (MICS) band at 402 MHz–405 MHz are already available, and the current research focus is on the optimization and miniaturization of the antenna [1], [2]. For cardiac pacemakers, higher data rates than the possible 800 kbit/s in the MICS band [3] are desirable in order to decrease the total power consumption, as the transmission of short data packets saves energy. High data rates are also valuable for other implanted devices, for instance, the retinal prosthesis [4] or the capsule endoscopy [5]. In the first case, a data telemetry link is set up between an extraocular device capturing an optical image and an intraocular implant with an electrode array stimulating the retinal ganglion cells in the eye. This prosthesis improves the vision of people with certain eye diseases. In the latter case, a camera is integrated in a capsule, which can be swallowed for medical diagnostics. After swallowing, the recorded images of the internal human body are transmitted wirelessly via an antenna to a base station placed outside the human body.

In contrast to narrow-band systems, ultra-wideband (UWB) systems provide the necessary high-data rates due to the inherent wide bandwidth and, therefore, cope with the increased complexity of the implanted devices described above. In addition, the simple structure of UWB transceivers leads to a low power consumption and low cost, both beneficial for implanted devices. These advantages are already demonstrated in a UWB transceiver applied for a cochlear implant [6]. Furthermore, if the FCC approved frequency range (3.1 GHz–10.6 GHz) is used, highly integrated systems are possible [7], and the antenna size can be reduced in comparison to systems operating in the MICS band. However, the design of broadband antennas is more challenging.

Tissue optimized UWB antennas are mainly investigated with respect to medical sensing applications like breast cancer detection [8]–[10] and vital signal monitoring [11], [12]. Therefore, these antennas have a directive behavior and are mostly bulky. Additionally, they are located outside the human body and are usually immersed in a low-loss liquid for the purpose of impedance matching to the human tissue. For short-range biotelemetry links with implants, hardly any UWB antennas are reported. In [13] at least simulative investigations are performed showing promising results. In this publication, a miniaturized planar UWB slot antenna is presented and optimized for operation in the human body. Therewith, a suitable candidate for implantation is provided. Beside the antenna design, the emphasis of the paper is on the characterization of the realized antenna in a lossy tissue mimic liquid.

II. Preliminary Investigations

A. Dielectric Properties of Human Tissue

In order to design an implantable antenna, the dielectric properties of human tissue has to be known. In [14] the complex permittivity is provided for several different human tissues in terms of a Cole-Cole expression [15]. In Fig. 1 and Fig. 2 the frequency-dependent results for the permittivity and the attenuation are plotted exemplarily for skin and muscle tissue. These results are established, however, a validation has been performed measuring the complex permittivity of the skin at different positions and for different persons. There, the coaxial probe method has been applied [16]. A typical result is shown in Fig. 1 and Fig. 2. The obtained lower value for the relative permittivity ε_r compared to the literature value [14] is confirmed by measurement results achieved in [17].

Implanted devices can be embedded around various tissues. For the design of the antenna, skin tissue is chosen for several reasons. Firstly, some devices, e. g., the cochlear implant, are implanted directly under the skin. Secondly, for implants placed around muscles, like the cardiac pacemaker, the dispersive behavior is similar to skin, and the difference

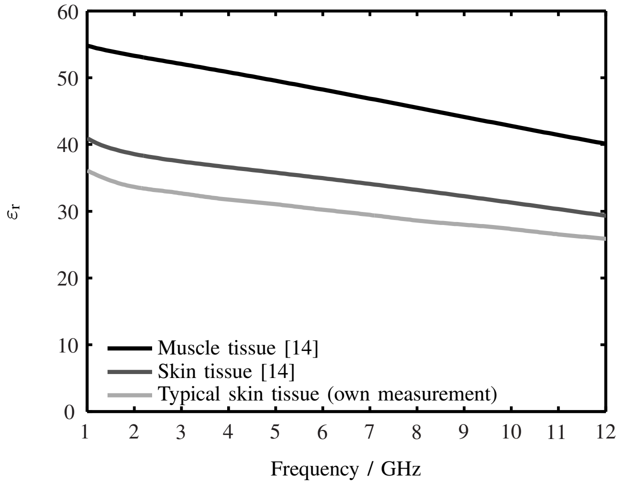

Fig. 1. Relative Permittivity ε_r of different human tissues.

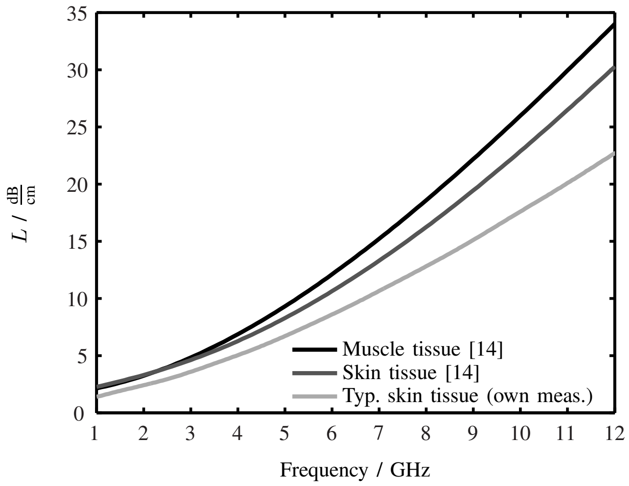

Fig. 2. Attenuation L of different human tissues.

in the ε_r value is relatively low compared to other tissues like fat ($\varepsilon_r \approx 5$). Furthermore, a first operational test can be easily performed with a hand-held antenna, and the antenna could be used for radiation in the human body, simply placing the antenna on the body. For the initial design of the antenna $\varepsilon_r = 28$ is used. This value corresponds to the ε_r value at 7 GHz of a typical skin tissue measurement.

B. Human Tissue Mimic Liquids

For characterization of an antenna (return loss and radiation pattern), a liquid is mandatory with similar dielectric properties like human tissue, which acts as tissue mimic. After investigation of several chemical substances, three candidates for a skin mimic were found: an acetone-water-solution (15% H_2O), a sugar-water-solution (50% H_2O) and a proprietary liquid basically consisting of oil and water (HSL5800, [18]). Their measured relative permittivity and attenuation L are given in Fig. 3 and Fig. 4, respectively. The attenuation has to be considered as it affects significantly the maximum ac-

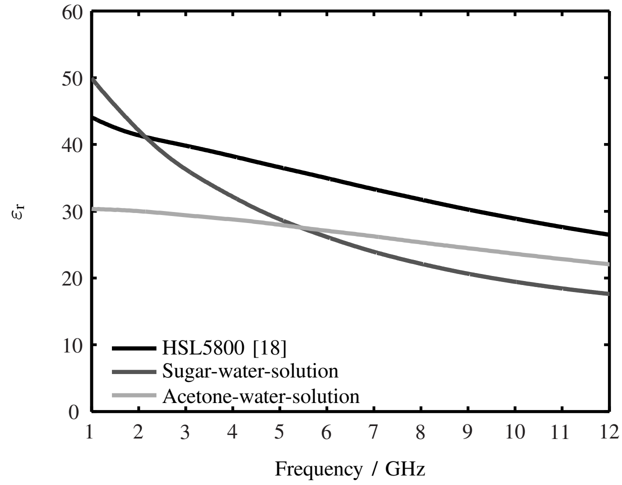

Fig. 3. Relative Permittivity ε_r of different suitable tissue mimic liquids.

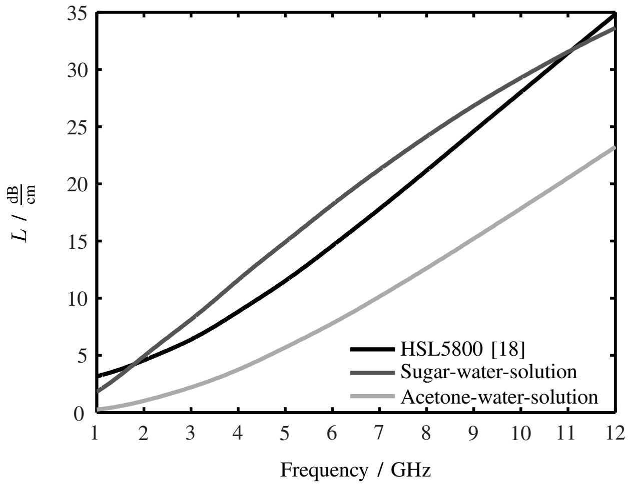

Fig. 4. Attenuation L of different tissue mimic liquids.

ceptable antenna distance for the measurement of the radiation pattern due to the highly lossy media. The pros and cons of these liquids for the radiation measurement are discussed in section IV-B.

III. Tissue Optimized Antenna

The basic element of the antenna is an elliptical slot in both ground planes of a triplate line leading to a UWB performance [19]. The slot is excited with an elliptical open stub as illustrated in Fig. 5. A triplate feeding line is used in order to insulate the feeding line from the surrounding highly lossy medium and to achieve a line impedance of $50\,\Omega$, independently of the permittivity of the surrounding medium. The three separate metal layers of the triplate line are shown in Fig. 6. The inner conductor is separated from the ground layers by two substrates having a height of 0.51 mm each. The chosen substrate material is RO4003 with $\varepsilon_r = 3.38$.

The dimensions of the elliptical stub and the slot aperture are optimized for a return loss of better than 10 dB in the

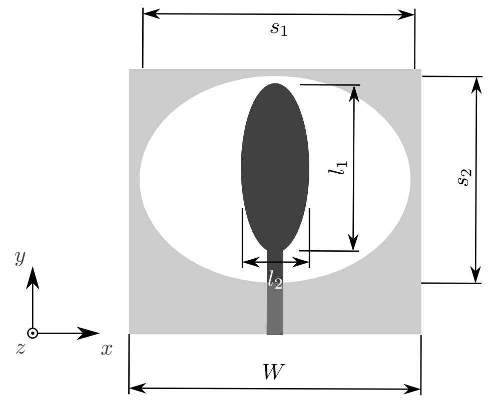

Fig. 5. Sketch of the triplate-fed slot antenna (top view).

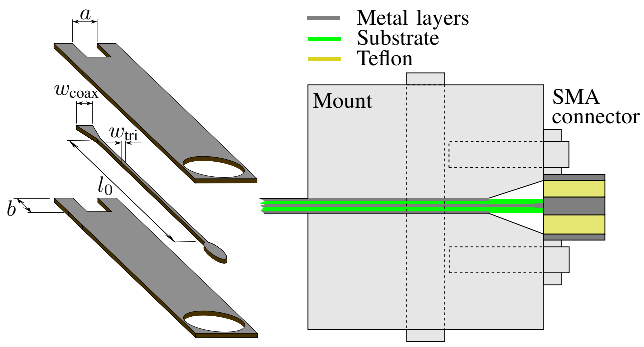

Fig. 6. Metallic layers of the antenna (left) and the antenna mount including the low-reflective transition from triplate line to coaxial line (right).

FCC frequency range, whereas a constant $\varepsilon_r = 28$ is assumed. The optimization was performed using Microwave Studio [20]. After optimization, the influence of a varying ε_r is investigated. As can be seen in Fig. 7, the return loss of the antenna element is little sensitive to ε_r variations.

A low-reflective transition from the triplate line to a coaxial line provides the connection to a SMA connector [21]. The transition is realized with a rectangular slot in both ground planes and a linear taper within the metallic antenna mount (see Fig. 6). The dimensions of the final design are summarized in Table I. Fig. 8 shows a photograph of the manufactured antenna with its remarkable small width of 11 mm.

TABLE I
DIMENSIONS OF THE ANTENNA ACCORDING TO FIG. 5 AND FIG. 6.

W	l_1	l_2	s_1	s_2
11.0 mm	6.35 mm	2.52 mm	10.2 mm	7.8 mm
a	b	l_0	w_{coax}	w_{tri}
4.375 mm	5.0 mm	38.18 mm	3.2 mm	0.565 mm

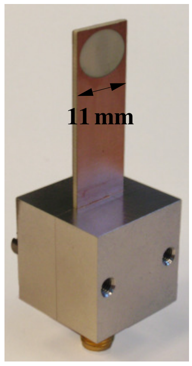

Fig. 8. Photograph of the manufactured antenna.

IV. Antenna Characterization in Lossy Liquid

A. *Return Loss*

The return loss of the realized antenna is measured, while the antenna is immersed in a tissue mimic liquid. For the three phantom liquids introduced previously–or if the antenna is enclosed by a human hand–similar results are obtained. As an example, the reflection coefficient is shown for the acetone solution in Fig. 9, together with the simulation result, whereas the measured frequency-dependent ε_r and L of acetone are applied for the simulation and the complete antenna structure

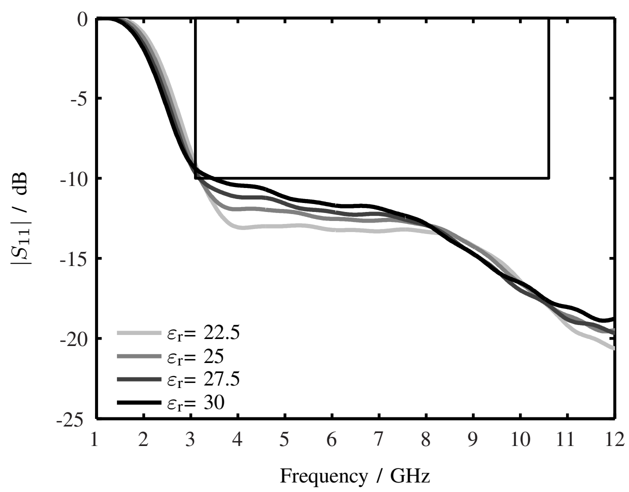

Fig. 7. Simulated matching performance for the radiating element with varying relative permittivity of the surrounding material.

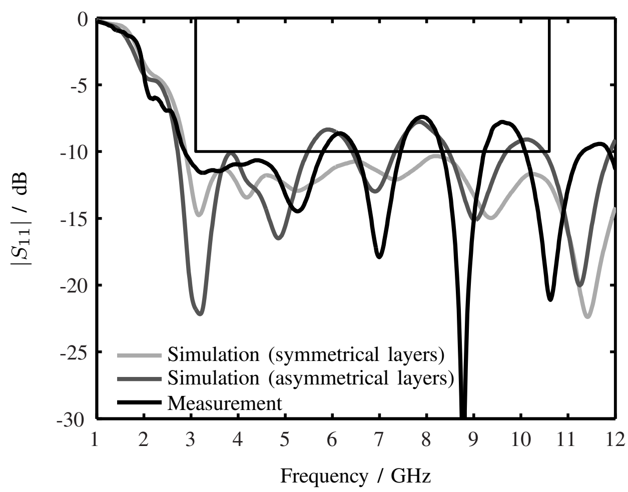

Fig. 9. Simulated and measured matching performance of the complete antenna structure including the transition to the coaxial line.

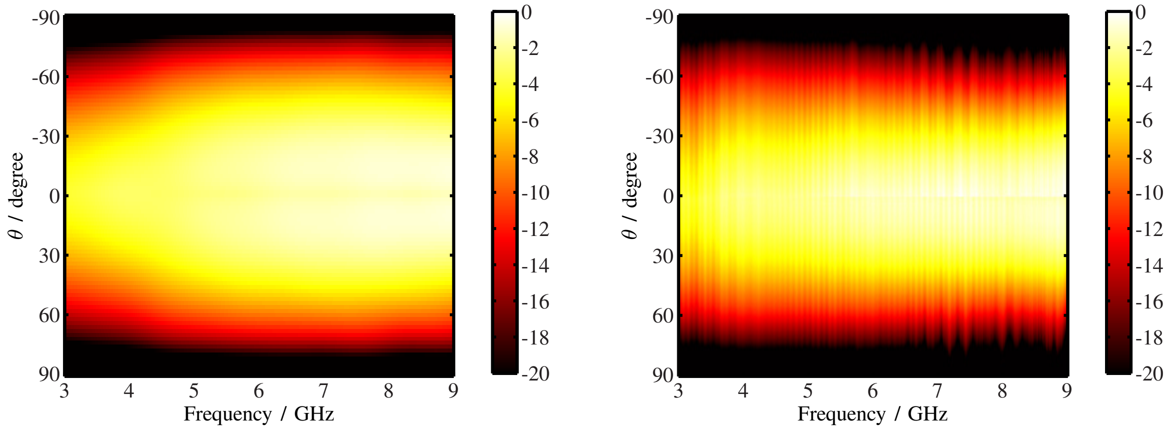

Fig. 11. Simulated (left) and measured (right) normalized radiation diagram for the E-plane in dB.

is taken into account. The measurement shows a higher ripple compared to the simulation leading to a return loss smaller than 10 dB within the frequency range 3.1 GHz–10.6 GHz. This ripple is probably caused by parallel plate modes propagating between the two ground planes of the triplate line. These modes are excited by an asymmetry within the triplate line, which is introduced by the fabrication of the triplate line glueing two substrates together. These modes are not present in the simulation, because an ideal symmetrical structure is assumed. If an asymmetry is artificially introduced in the simulation, also a higher ripple is obtained (see Fig. 9). For a revised design of the antenna, it is intended to suppress these parasitic modes with proper positioned vias.

B. Radiation Pattern

In order to determine the radiation performance, two identical antennas are placed within a tank filled with a homogeneous tissue mimic liquid. Then, one antenna is rotated and the transmission is recorded using a vectorial network analyzer (VNWA). For automation, the rotation is performed with a stepper motor. The complete setup is shown in the photograph in Fig. 10.

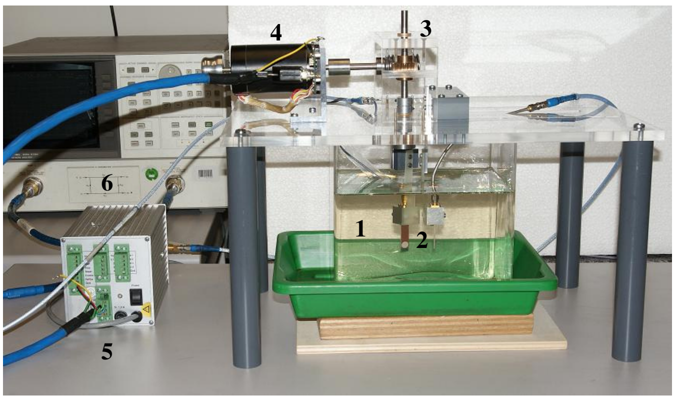

Fig. 10. Photograph of the radiation pattern measurement setup (**1** tank filled with sugar solution, **2** immersed antennas, **3** axis and gear, **4** stepper motor, **5** motor controller, **6** VNWA).

For the use as a tissue mimic liquid, the previously described liquids are under consideration. Regarding the frequency behavior of ε_r and the attenuation, the acetone solution achieves the best performance and is therefore best suited. However, acetone is easily flammable, irritant and exhalable and has to be handled with care, especially in high volume. The ε_r value of HSL5800 is above the targeted value, and due to its high opacity the radiation pattern measurement is more complicated. Therefore, the sugar solution has been chosen for the first measurement of the radiation pattern, albeit the sugar solution has the most dispersive behavior and the highest attenuation.

The measured and simulated normalized radiation pattern are shown in Fig. 11 and Fig. 12 for the E-plane (y-z-plane) and H-plane (x-z-plane), respectively, with the antennas immersed in sugar solution. Due to the increased losses of the sugar solution at high frequencies, only results up to 9 GHz could be recorded. For the measured patterns in Fig. 11 and Fig. 12, the frequency-dependent material loss is compensated for a better visualization and comparison with the simulation result. The obtained radiation patterns agree quite well with the simulation, taking into account that for the simulation the value of ε_r is assumed as constant, whereas the liquid in the measurement setup is very dispersive. In the H-plane, an asymmetry in the radiation pattern is obtained in contrast to the simulated diagram. This effect is probably caused by a slight misalignment of the feeding stub during the antenna fabrication process. The measured mean gain of the antenna is 3.8 dBi.

V. Conclusion

A small triplate-fed UWB slot antenna capable for operation in human tissue is proposed and evaluated in a human tissue mimic liquid in the FCC frequency range 3.1 GHz–10.6 GHz. The return loss and the radiation pattern of the antenna show promising results and confirm the usability for an implanted device like a cardiac pacemaker or a cochlear implant.

In future, after validation in different phantom liquids, the antenna will be optimized for the suppression of parallel plate modes. More care has to be spent on a precise fabrication.

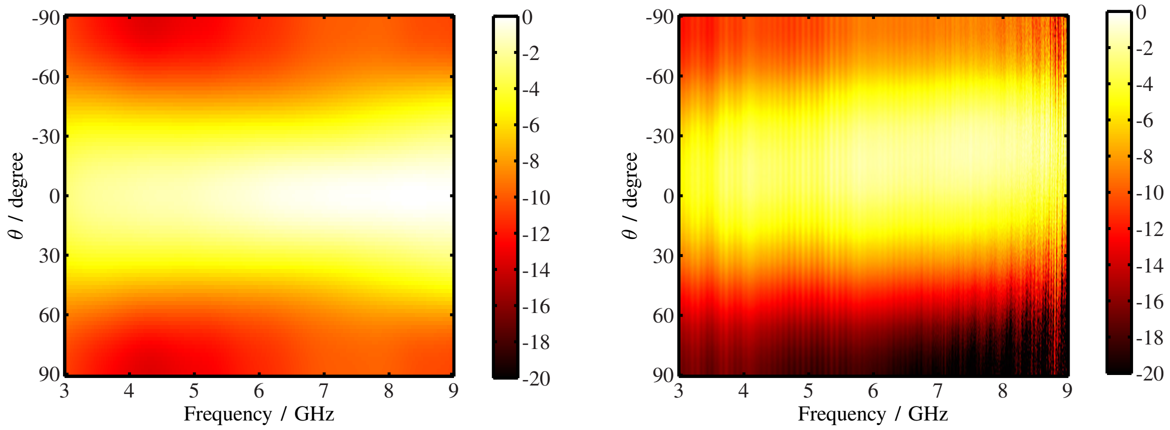

Fig. 12. Simulated (left) and measured (right) normalized radiation diagram for the H-plane in dB.

Then, it is intended to verify the transmission from this antenna immersed in a phantom liquid (implanted device) to an antenna outside the liquid (base station). The final step will be the optimization of the antenna for a specific application with a defined surrounding tissue and the usage of ceramic substrates or superstrates in order to achieve a biocompatible antenna.

ACKNOWLEDGMENT

This work has been funded by the German Research Foundation (DFG) under the program UKoLoS.

REFERENCES

[1] J. Kim and Y. Rahmat-Samii, "Implanted antennas inside a human body: simulations, designs, and characterizations," *IEEE Transactions on Microwave Theory and Techniques*, vol. 52, no. 8, pp. 1934–1943, Aug. 2004.

[2] P. Soontornpipit, C. Furse, and Y. C. Chung, "Design of implantable microstrip antenna for communication with medical implants," *IEEE Transactions on Microwave Theory and Techniques*, vol. 52, no. 8, pp. 1944–1951, Aug. 2004.

[3] P. Bradley, "An ultra low power, high performance medical implant communication system (MICS) transceiver for implantable devices," in *IEEE Biomedical Circuits and Systems Conference*, Nov. 2006, pp. 158–161.

[4] K. Gosalia, G. Lazzi, and M. Humayun, "Investigation of a microwave data telemetry link for a retinal prosthesis," *IEEE Transactions on Microwave Theory and Techniques*, vol. 52, no. 8-2, pp. 1925–1933, Aug. 2004.

[5] S. H. Lee and Y. J. Yoon, "A dual spiral antenna for ultra-wideband capsule endoscope system," in *International Workshop on Antenna Technology (iWAT)*, Mar. 2008, pp. 227–230.

[6] T. Buchegger, G. Oßberger, A. Reisenzahn, E. Hochmaier, A. Stelzer, and A. Springer, "Ultra-wideband transceivers for cochlear implants," *EURASIP Journal on Applied Signal Processing*, vol. 18, pp. 3069–3075, Jan. 2005.

[7] J. Dederer, B. Schleicher, A. Trasser, T. Feger, and H. Schumacher, "A fully monolithic 3.1-10.6 GHz UWB Si/SiGe HBT impulse-UWB correlation receiver," in *IEEE International Conference on Ultra-Wideband*, vol. 1, Sep. 2008, pp. 33–36.

[8] R. Nilavalan, I. Craddock, A. Preece, J. Leendertz, and R. Benjamin, "Wideband microstrip patch antenna design for breast cancer tumor detection," *IET Microwaves, Antennas & Propagation*, vol. 1, no. 2, pp. 277–281, Apr. 2007.

[9] D. R. Gibbins, M. Klemm, I. J. Craddock, G. S. Hilton, and D. L. Paul, "The design of wide slot antenna for the transmission of UWB signals into the human body using FDTD simulation," in *European Conference on Antennas and Propagation*, Nov. 2007, pp. 1–5.

[10] M. H. Shenouda and E. C. Fear, "Design of dielectric immersed tapered slotline antenna for radar-based microwave breast imaging," *Microwave and Optical Technology Letters*, vol. 51, no. 3, pp. 633–638, Mar. 2009.

[11] U. Schwarz, M. Helbig, J. Sachs, F. Seifert, R. Stephan, F. Thiel, and M. Hein, "Physically small and adjustable double-ridged horn antenna for biomedical UWB radar applications," in *IEEE International Conference on Ultra-Wideband*, vol. 1, Sep. 2008, pp. 5–8.

[12] M. Leib, E. Schmitt, A. Gronau, J. Dederer, B. Schleicher, H. Schumacher, and W. Menzel, "A compact ultra-wideband radar for medical applications," *Frequenz*, vol. 63, no. 1-2, pp. 1–8, Feb. 2009.

[13] A. Khaleghi and I. Balasingham, "Improving in-body wideband communication using near-field coupling of the implanted antenna," *Microwave and Optical Technology Letters*, vol. 51, no. 3, pp. 585–589, Mar. 2009.

[14] S. Gabriel, R. W. Lau, and C. Gabriel, "The dielectric properties of biological tissues: III. parametric models for the dielectric spectrum of tissues," *Phys. Med. Biol.*, vol. 41, no. 11, pp. 2271–2293, Nov. 1996.

[15] K. S. Cole and R. H. Cole, "Dispersion and absorption in dielectrics," *Journal of Chemical Physics*, vol. 9, pp. 341–351, Apr. 1941.

[16] Y. Wei and Y. Sridhar, "Technique for measuring the frequency-dependent complex dielectric constants of liquids up to 20 GHz," *Review of Scientific Instruments*, vol. 60, no. 9, pp. 3041–3046, Sep. 1989.

[17] U. Schwarz, M. Helbig, R. Stephan, J. Sachs, and M. A. Hein, "Ultrabreitbandantennen für biomedizinische Anwendungen," in *Kleinheubacher Tagung*, 2007.

[18] Schmid & Partner Engineering AG (Speag), "Tissue simulating liquids: HSL5800," 2008.

[19] E. S. Angelopoulos, A. Z. Anastopoulos, D. I. Kaklamani, A. A. Alexandridis, F. Lazarakis, and K. Dangakis, "Circular and elliptical cpw-fed slot and microstrip-fed antennas for ultrawideband applications," *IEEE Antennas and Wireless Propagation Letters*, vol. 5, no. 1, pp. 294–297, Dec. 2006.

[20] *Microwave Studio*, CST - Computer Simulation Technology, Version 2008.

[21] R. Leberer, "Untersuchung von quasi-planaren Antennen mit sektorförmiger und omnidirektionaler Strahlungscharakteristik im Millimeterwellenbereich," Ph.D. dissertation, University of Ulm, Institute for Microwave Techniques, Jul. 2005.